Rotating and Fugitive Cavity Solitons in semiconductor microresonators

R. Kheradmand[1], **L. A. Lugiato and G. Tissoni**

INFM, Dipartimento di Scienze Chimiche, Fisiche e Matematiche, Università dell'Insubria, via Valleggio 11, 22100 Como, Italy

M. Brambilla

INFM, Dipartimento di Fisica Interateneo, Università e Politecnico di Bari, via Orabona 4, 70126 Bari, Italy

H. Tajalli

[1]*Center for Applied Physics and Astronomical Research, University of Tabriz, Tabriz 51664-163, Iran*

Abstract: We describe two different methods that exploit the intrinsic mobility properties of cavity solitons to realize periodic motion, suitable in principle to provide soliton-based, all-optical clocking or synchronization. The first method relies on the drift of solitons in phase gradients: when the holding beam corresponds to a doughnut mode (instead of a Gaussian as usually) cavity solitons undergo a rotational motion along the annulus of the doughnut. The second makes additional use of the recently discovered spontaneous motion of cavity solitons induced by the thermal dynamics, it demonstrates that it can be controlled by introducing phase or amplitude modulations in the holding beam. Finally, we show that in presence of a weak 2D phase modulation, the cavity soliton, under the thermally induced motion, performs a random walk from one maximum of the phase profile to another, always escaping from the temperature minimum generated by the soliton itself (Fugitive Soliton).

OCIS codes: (190.4420) Nonlinear optics, transverse effects in; (190.4870) Optically induced thermo-optical effects; (160.6000) Semiconductors, including MQW

References and links

1. D. W. McLaughlin, J. V. Moloney and A. C. Newell, "Solitary Waves as Fixed Points of Infinite-Dimensional Maps in an Optical Bistable Ring Cavity," Phys. Rev. Lett. **51**, 75-78 (1983).
2. N. N. Rosanov and G. V. Khodova, "Autosolitons in bistable interferometers," Opt. Spectrosc. **65**, 449-450 (1988).
3. G. S. McDonald, and W. J. Firth "Spatial solitary wave optical memory," J. Opt. Soc. Am. B **7**, 1328-1335 (1990).
4. M. Tlidi, P. Mandel and R. Lefever, "Localized structures and localized patterns in optical bistability," Phys. Rev. Lett. **73**, 640-643 (1994).
5. For review, see L. A. Lugiato, "Introduction to the Special Issue on Cavity Solitons," IEEE J. Quant. Electron.**39**, 193 (2003)
6. For review, see W. J. Firth and G. K. Harkness, "Existence, Stability and Properties of Cavity Solitons," in "Spatial Solitons," Springer Series in Optical Sciences Vol. 82, eds. S. Trillo and W. Torruellas, pp. 343-358 (Springer Velag, 2002).
7. W. J. Firth and A. J. Scroggie, "Optical bullet holes: robust controllable localized states of a nonlinear cavity," Phys. Rev. Lett. **76**, 1623-1626 (1996).
8. M. Brambilla, L. A. Lugiato, F. Prati, L. Spinelli and W. J. Firth,"Spatial soliton pixels in semiconductor devices," Phys. Rev. Lett. **79**, 2042 (1997).

#3247 - $15.00 US Received October 30, 2003; Revised December 19, 2003

9. D. Michaelis, U. Peschel and F. Lederer, "Multistable localized structures and superlattices in semiconductor optical resonators," Phys. Rev. A **56**, R3366-R3369 (1997).
10. L. Spinelli, G. Tissoni, M. Brambilla, F. Prati and L. A. Lugiato, "Spatial solitons in semiconductor microcavities," Phys. Rev. A **58**, 2542-2559 (1998) and references quoted therein.
11. G. Tissoni, L. Spinelli, M. Brambilla, T. Maggipinto, I. Perrini and L. A. Lugiato, "Cavity solitons in passive bulk semiconductor microcavities. I. Microscopic model and modulational instabilities," J. Opt. Soc. Am. B **16**, 2083 (1999).
12. L. Spinelli, G. Tissoni, M. Tarenghi and M. Brambilla, "First principle theory for cavity solitons in semiconductor microresonators," Eur. Phys. J. D **15**, 257-266 (2001) and references quoted therein.
13. S. Barland, J. R. Tredicce, M. Brambilla, L. A. Lugiato, S. Balle, M. Giudici, T. Maggipinto, L. Spinelli, G. Tissoni, T. Knoedl, M. Miller and R. Jaeger,"Cavity Solitons as pixels in semiconductor microcavities," Nature **419**, 699-702 (2002).
14. L. Spinelli, G. Tissoni, L. A. Lugiato and M. Brambilla, "Thermal effects and transverse structures in semiconductor microcavities with population inversion," Phys. Rev. A **66**, 023817 (2002).
15. A. J. Scroggie, J. M. McSloy, and W. J. Firth, "Self-propelled cavity solitons in semiconductor microcavities," Phys. Rev. E**66**, 036607 (2002).
16. G. Tissoni, L. Spinelli and L. A. Lugiato,"Spatio-temporal dynamics in semiconductor microresonators with thermal effects," Opt. Ex. **10**, 1009 (2002).
17. I. M. Perrini, G. Tissoni, T. Maggipinto, and M. Brambilla, "Thermal effects and cavity solitons in passive semiconductor microresonators," submitted to J. Opt. B (2003).
18. D. V. Skryabin, A. Yulin, D. Michaelis, W. J. Firth, G-L. Oppo, U. Peschel and F. Lederer, "Perturbation Theory for Domain Walls in the Parametric Ginzburg-Landau Equation," Phys. Rev. E **64**, 56618-1-9 (2001).
19. L. Allen, M. W. Beijersbergen, R. J. C. Spreuw and J. P. Woerdman, "Orbital angular momentum of light and the transformation of Laguerre-Gaussian laser modes," Phys. Rev. A **45**, 8185-8189 (1992).
20. L. Allen, S. M. Barnett and M. J. Padgett, "Optical angular Momentum," Institute of Physics Publishing, Bristol, (2003).
21. B. Sfez, J. L. Oudar, J. C. Michel, R. Kuszelewicz and R. Azoulay, "High contrast multiple quantum well optical bistable device with integrated Bragg reflectors," Appl. Phys. Lett. **57**, 324 (1990).
22. B. Sfez, J. L. Oudar, J. C. Michel, R. Kuszelewicz and R. Azoulay, "External-beam switching in monolithic bistable GaAs quantum well etalons," Appl. Phys. Lett. **57**, 1849 (1990).
23. W. J. Firth and G. Harkness, "Cavity Solitons," Asian J. Phys. **7**, 665-677 (1998).
24. G. Tissoni, L. Spinelli, M. Brambilla, T. Maggipinto, I. Perrini and L. A. Lugiato, "Cavity solitons in passive bulk semiconductor microcavities. II. Dynamical proprties and control," J. Opt. Soc. Am. B **16**, 2095 (1999).
25. T. Maggipinto, M. Brambilla, G. K. Harkness and W. J. Firth, "Cavity Solitons in Semiconductor Microresonators: Existence, Stability and Dynamical Properties," Phys Rev E **62**, 8726-8739 (2000).
26. G-L. Oppo, A. J. Scroggie and W. J. Firth, "Characterization, Dynamics and Stabilization of Diffractive Domain Walls and Dark Ring Cavity Solitons in Optical Parametric Oscillators," Phys Rev E **63** 066209-1/15 (2001).

1. Introduction

Cavity solitons (CSs) [1, 2, 3, 4, 5, 6, 7, 8] are stationary bright/dark 1-peak localised structures over a homogeneous background in the section of broad radiation beams. The possibility of switching them on/off, controlling their location and their motion makes them interesting as pixels for reconfigurable arrays or all-optical processing units [7, 8].

Most interesting from the practical viewpoint, for miniaturization purposes, is the case in which the active medium is a semiconductor: the standard configuration on which we will focus our attention is that of an optical cavity containing a semiconductor medium and driven by a stationary holding beam (HB); both the material sample and the holding beam have a large section.

Phenomenological models [8, 9, 10] have been proposed to describe the semiconductor material; on the other hand, a more accurate modelization of the semiconductor materials, including a microscopic description of the optical nonlinearity has been performed in [11, 12]. CSs have been recently experimentally demonstrated in semiconductor amplifiers [13].

The analysis of this paper concerns and combines two different issues in the physics of cavity solitons.

1) Motion of CSs induced by the presence of phase/amplitude gradients in the holding beam.

2) Spontaneous motion of CSs induced by the slow thermal dynamics. This phenomenon

#3247 - $15.00 US Received October 30, 2003; Revised December 19, 2003

was predicted in [14] for the case of a driven VCSEL with population inversion, extended to the 2D case in [15] and [16], and extended to a configuration without population inversion in [15, 17]. It is caused by the circumstance that the temperature field evolves with a time scale much larger than that of the carrier field and of the electric field. In an appropriate parameter range, this gives rise to a pitchfork bifurcation [15, 18] which induces a spontaneous motion of patterns and of CSs. When the CS is switched on, the optical spot remains stationarily in the location where it was created for times shorter than the time scale (microsecond) which characterizes the thermal dynamics, then it starts moving in a random direction; after an initial transient, the velocity becomes constant when the holding beam (HB) is flat. When several CSs are present, they move, in general, in different directions. The destabilization process arises in the following way: after excitation of the CS, a minimum appears in the temperature profile, at the spatial location of the optical spot. This is a consequence of the fact that a maximum of intensity corresponds to less carriers and less heating (in active systems). When the temperature in the minimum reaches a certain critical value, the optical spot starts moving towards larger values of temperature [16]. The minimum of the temperature profile gradually disappears and a dynamical equilibrium is reached, in which the optical spot and the temperature front move together (see Fig. 4 of [16]).

Our analysis is subdivided into two parts of unequal lengths

a) The first part concerns only point 1) and is based on a model which does not include the temperature. Up to now, the effects of gradients in the HB have been mainly studied by introducing a phase modulation in a plane-wave HB [7], or an amplitude modulation which converts the plane-wave configuration of the HB into a Gaussian one [10]. Here we consider the case of a doughnut-shaped holding beam, which is both amplitude and phase-modulated, and show that - as one can easily understand - one has a uniform rotational motion of CSs along the annulus of the doughnut. This is the paradigmatic configuration of a HB which gives rise to a rotatory motion. In addition, this is a visual demonstration of the orbital angular momentum carried by the doughnut mode [19, 20].

b) The second part is based on a model which includes the temperature dynamics and we analyze how the presence of phase/amplitude gradients affects the spontaneous motion described above in point 2). Such a motion represents in principle a problem but, as we show, can be controlled by gradients and this feature may open new opportunities for application. In [14] our analysis was limited to the case of one transverse dimension and we showed that in 1D the spontaneous motion can be confined or even suppressed by introducing a phase modulation. In 2D there is a far richer scenario of possibilities for example, Ref. [15] illustrates the collision between two dark CSs in the passive (i. e. without population inversion) case. Here we examine some of the simplest and most meaningful configurations.

2. The model

2.1. a) Without thermal effects

We consider a broad area semiconductor heterostructure in both the active (i.e., with population inversion) and the passive configuration. The semiconductor microresonator is of the Fabry-Perot type, with a MQW structure perpendicular to the direction z of propagation of the radiation inside the cavity as in [10]. The dynamical equations for the slowly varying coherent field and carrier density, in the paraxial and mean field limit approximations, are:

$$\frac{\partial E}{\partial t} = -\kappa\left[(1+\eta+\mathrm{i}\theta)E + E_I - 2C\mathrm{i}\Theta(N-1)E + \mathrm{i}\nabla_\perp^2 E\right], \quad (1)$$

$$\frac{\partial N}{\partial t} = -\gamma_\parallel\left[N + \beta N^2 - I + (N-1)|E|^2 - d\nabla_\perp^2 N\right], \quad (2)$$

#3247 - $15.00 US Received October 30, 2003; Revised December 19, 2003

where E, N are the normalized electric field and the carrier density normalized to the transparency value, respectively, κ is the cavity damping constant, $\gamma_\parallel$ is the carrier nonradiative recombination rate, $\theta = (\omega_c - \omega_0)/\kappa$ is the cavity detuning parameter, with ω_0 being the frequency of the holding field and ω_c the longitudinal cavity frequency closest to ω_0. The transverse Laplacian, defined as usual as $\nabla_\perp^2 = \partial^2/\partial x^2 + \partial^2/\partial y^2$, represents diffraction (in Eq. 1), and carrier diffusion (in Eq. 2 through the diffusion parameter d), η is proportional to the linear absorption coefficient per unit length due to the material in the region between the QWs and the reflectors, $\beta = BN_0/\gamma_\parallel$ where B is the coefficient of radiative recombination involving two carriers, N_0 is the carrier density at transparency. The transverse coordinates x and y are scaled to the diffraction length. The parameter E_I is the normalized injected field (taken real and positive for definiteness), I is the normalized injected current, C is the bistability parameter.

In the passive configuration $\Theta = (\Delta + i)/(1 + \Delta^2)$ and $\Delta = (\omega_e - \omega_0)/\gamma_e$, where ω_e is the central frequency of the excitonic absorption line, approximated by a Lorentzian curve, and γ_e is the half-width of the excitonic line. In the active configuration $\Theta = \alpha + i$, where α is the line-width enhancement factor typical of semiconductor lasers.

In order to perform an analysis as realistic as possible in comparison with the devices nowadays available, the choice of numerical values of the physical quantities characterizing our model was inspired by some experimental works on optical bistability in GaAs MQW structures [21, 22]. The reader is referred to Ref. [10] for a more detailed discussion of the model equations and of the calculations of the homogeneous stationary solutions and their stability analysis.

2.2. b) Including thermal effects

The device is essentially the same as in case **a)**, but here we also take into account the thermal dynamics.

The time evolution of the system can be described by considering an additional equation for the lattice temperature T, that is coupled to the field and carrier equations through the temperature dependence of the nonlinear susceptibility and of the cavity detuning parameter (see [14, 15]) :

$$\frac{\partial E}{\partial t} = -\kappa \left[(1 + \mathrm{i}\theta(T))E - E_I - \mathrm{i}\Sigma\chi_{nl}(N, T, \omega_0)E - \mathrm{i}\nabla_\perp^2 E \right], \tag{3}$$

$$\frac{\partial N}{\partial t} = -\gamma_\parallel \left[N - \mathrm{Im}\left(\chi_{nl}(N, T, \omega_0)\right)|E|^2 - I - d\nabla_\perp^2 N \right], \tag{4}$$

$$\frac{\partial T}{\partial t} = -\gamma_{th} \left[(T - 1) - D_T \nabla_\perp^2 T \right] + \gamma Z N + \gamma P I^2, \tag{5}$$

where T is the lattice temperature normalized to the room temperature T_0, γ_{th} is its decay rate towards the environmental temperature.

The coefficients Z and P describe the heating of the device due to carriers and to Joule effect, respectively.

In order to take into account the thermal shift of the cavity frequency in this model, we have considered a linear dependence on temperature in the cavity detuning θ, this effect being related to the material layers in the regions between the nonlinear medium and the reflectors:

$$\theta = \theta_0 - \lambda(T - 1), \tag{6}$$

with

$$\lambda = \frac{4\pi T_0}{n\Gamma} \frac{\partial n}{\partial T}, \tag{7}$$

#3247 - $15.00 US Received October 30, 2003; Revised December 19, 2003

where θ_0 is the cavity detuning at room temperature, n is the background refractive index, $\frac{\partial n}{\partial T} \simeq 10^{-4}K^{-1}$ and Γ is the mean value of the mirror transmissivity. For a full description of the system parameters of the homogeneous steady state and its linear stability analysis we refer to [14]. As for the nonlinear susceptibility χ_{nl}, as in [14] we adopt the microscopic description of [12] to include the bandgap shift upon an increase of temperature.

3. Numerical Analysis

The numerical integration of dynamical equations was performed by using a split-step method with periodic boundary conditions. This method implies the separation of the algebraic and the Laplacian terms in the right-hand side of dynamical equations. The first part is integrated via a Runge-Kutta algorithm, while the linear operator (Laplacian) is integrated via a FFT algorithm.

In both previous models *a*) and *b*), when the input filed E_I is a plane-wave (i.e. it does not depend on the transverse variables x and y) the dynamical equations admit homogeneous (i.e. x-and y-independent) stationary solutions. In all cases considered in this paper, the steady-state curve of $|E_S|$, where E_S is the stationary value of the field E, as a function of E_I is S-shaped (see e.g. Fig. 2 and 4 in the following) and its lower branch is stable. On the contrary, the negative-slope branch and part of the upper branch are unstable against the growth of spatially modulated perturbations.

3.1. a) Without thermal effects

We studied Eqs. (1) and (2) both in the passive and in the active configurations. In the passive case, we set $I = 0$, $\eta = 0.25$, $\beta = 1.6$, $d = 0.2$ and $\Delta = -1$. The values are derived from Ref. [10]. As for the remaining parameters, we chose $\theta = -3$ and $C = 40$.

Initially, we switch a CS on by exploiting the usual superposition of a narrow gaussian pulse on top of the plane-wave holding beam. After the CS formation we change the holding beam configuration by introducing a phase/amplitude modulation. Precisely, we convert the plan-wave HB into a Gauss-Laguerre doughnut mode (TEM^*_{10} or TEM^*_{01}), as shown in Fig. 1(a).

The CS moves towards the circle where the annulus of the doughnut mode is maximum (as usually, CSs tend to the local maxima of the amplitude profile) and remains trapped there. In addition, the CS experiences a force due to the phase modulation $exp(\pm i\varphi(x,y))$ (with $\varphi(x,y) = \tan^{-1}(\frac{y}{x})$) of the doughnut mode which causes a rotational motion (see the movie in Fig. 1(b)) along the circle. The sense of rotation is determined by the helicity (or equivalently, by the orbital angular momentum) of the HB and is counter-clockwise (clockwise) in the $+(-)$ case. We studied also the active configuration, where the device is pumped by an injected current I larger than the transparency value I_0, in such a way that it becomes an amplifier, slightly below the threshold for laser emission, with an injected field E_I.

Again, we adopt numerical values derived from Ref. [10]. In this case, the threshold current is $I_{th} = 2.11$, and we set $I = 2$. We considered the parameter $\alpha = 5$, $\theta = -2$, $C = 0.45$, $\eta = \beta = 0$ and $d = 0.052$. In Fig. 2 we show the steady-state curve, the dotted segment is unstable because of a modulational instability. We consider values of E_I just below the righthand turning point of the **S**-shaped curve, so that the presence of CSs is observed. We create a pair of cavity solitons, then we change the plane-wave HB into a doughnut-mode as before. Fig. 3 shows a movie in which the two CSs rotate in the same direction.

In the active configuration we measured the velocity of cavity solitons in presence of a doughnut mode with phase modulation $\exp(\pm i\varphi)$ and we got $v = 2.02\mu m/nsec$, while by changing $\exp(\pm i\varphi)$ into $\exp(\pm 2i\varphi)$ we got $v = 2.2\mu m/nsec$. Hence, the cavity soliton velocity does not seem to be significantly affected. This is only apparently in contrast with the predicted linear dependence of the drift speed on the field gradient [23, 24, 25], because the linear relation holds when the field phase gradient can be treated perturbatively. In this case, the doughnut having

#3247 - $15.00 US Received October 30, 2003; Revised December 19, 2003

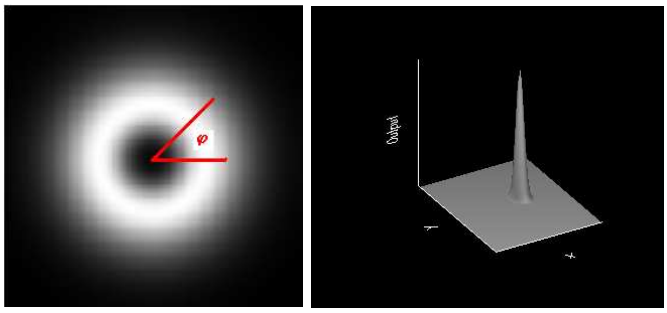

Fig. 1. Gauss-Laguerre mode (TEM^{*}_{10}) that we used as holding beam (a). The movie (b) shows the rotatory motion of CS due to the phase profile $e^{+i\varphi}$ of the holding beam. Passive configuration, without thermal effects. Parameters are: $\kappa^{-1} = 10ps$, $\gamma_{\|}^{-1} = 10ns$, $I = 0$, $\eta = 0.25$, $\beta = 1.6$, $d = 0.2$, $\theta = -3$, $C = 40$, $\Delta = -1$.

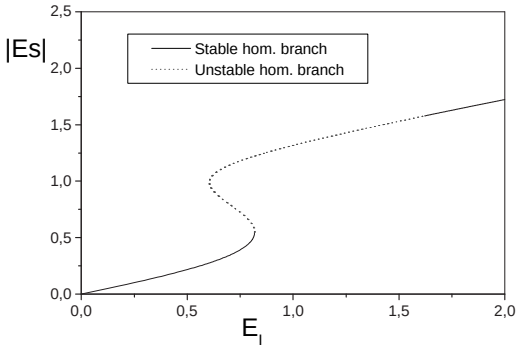

Fig. 2. Active configuration without thermal effects: steady-state curve. Parameters are: $C = 0.45$, $\theta = -2$, $\alpha = 5$, $I = 2$, $\eta = 0$, $\beta = 0$ and $d = 0.052$.

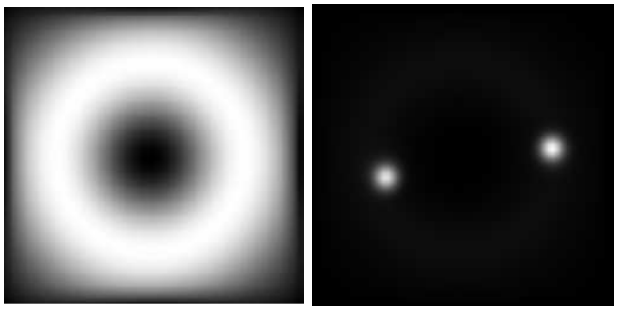

Fig. 3. Gauss-Laguerre mode (TEM^{*}_{01}) that we used as holding beam (a). The movie (b) shows the rotatory motion of 2 CSs due to the phase profile $e^{-i\varphi}$ of the holding beam. Active configuration, without thermal effects. Temporal parameters are: $\kappa^{-1} = 10ps, \gamma^{-1} = 1ns$. Other parameters are as in Fig. 2.

#3247 - $15.00 US
Received October 30, 2003; Revised December 19, 2003

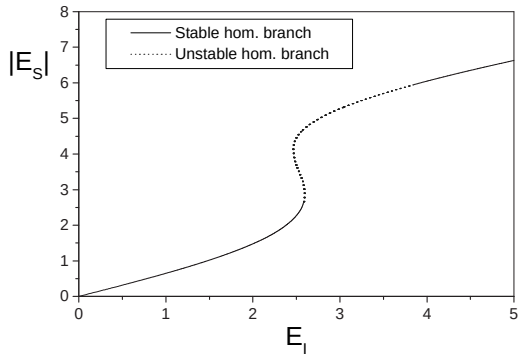

Fig. 4. Active configuration with thermal effects: steady-state curve. Parameters are: $\kappa^{-1} = 10ps, \gamma_{\parallel}^{-1} = 1ns, \gamma_{th}^{-1} = 1\mu s$, $D_T = 1, d = 0.1, \Delta = 3, \theta_0 = -18.5, \Sigma = 80, Z \simeq 1.2 \cdot 10^{-4}, P \simeq 8.1 \cdot 10^{-8}, I = 1.43$.

a unitary phase pitch, this is far from true. Moreover, we expect that for high CS velocity, the carrier dynamics slows down the motion, thus providing a saturation effect in the drift speed.

We want to make further investigations on this topic to evaluate more finely the speed dependence on the phase gradient and on the injected field amplitude, in order to quantify the saturation. We leave this calculations for a future publication.

In Ref. [26], dealing with a different kind of cavity solitons (Dark Ring Cavity Solitons) that exist in an optical parametric oscillator, the rotation of a domain wall on a doughnut beam is analysed, with very good quantitative agreement between analysis and the simulations for the rotation speed of the domain wall.

3.2. b) Including thermal effects

We solve numerically Eqs. (3-5) to demonstrate that the spontaneous drift of CSs, induced by thermal effects, can be controlled by using a HB with appropriate phase/amplitude modulation.

As for the parameter set, we refer the reader to the case reported in [14], setting $Z \simeq 1.2 \times 10^{-4}$, $P \simeq 8.1 \times 10^{-8}$, $\Sigma = 80$, $\Delta = 3$, $\theta_0 = -18.5$, $I = 1.43$, $d = 0.1$ and $D_T = 1$. The homogeneous stationary solution is shown in Fig. 4, where the dotted segment is unstable because of a dynamical modulational instability, which indicates the drift of CSs.

We note that for a different choice of the parameter set, in particular of the diffusion parameters, an opposite situation can take place, and stationary CSs can be found [14].

We switch a CS on for $E_I = 2.55$, where the lower branch of the steady-state curve is stable. We remove the writing pulse and the optical spot persists in the position where it has been excited for an initial interval time on the order of γ_{th}^{-1}, and then it starts drifting in a random direction.

We decided to control the direction of motion by introducing a phase or an amplitude modulation in the holding beam.

In the case of phase modulation, we superimpose to the homogeneous HB two orthogonal standing waves of amplitudes ρ_1 and ρ_2, respectively, and out of phase by $\frac{\pi}{2}$ with respect to the homogeneous background; so that [10]

$$E_I(x,y) = E_I^{(0)}[1 + i(\varepsilon_1 cosKx + \varepsilon_2 cosKy)], \tag{8}$$

where $\varepsilon_i = 2\rho_i/E_I^{(0)}$(i=1,2). Provided that ε_i is sufficiently small, E_I acquires essentially a pure

#3247 - $15.00 US Received October 30, 2003; Revised December 19, 2003

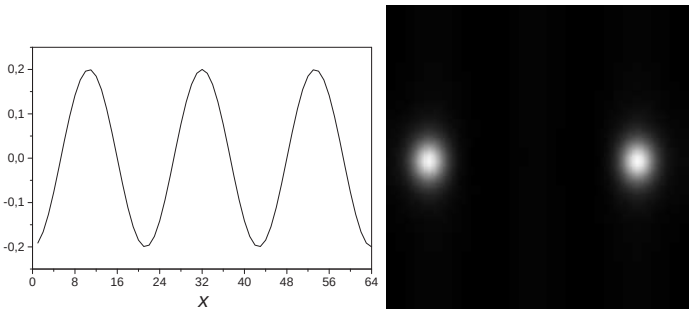

Fig. 5. 1D phase profile of the holding beam (a). The movie (b) shows the dynamics of two CSs. Parameters are as in Fig. 4.

phase modulation, becoming

$$E_I(x,y) \approx E_I^{(0)} exp(i\varphi(x,y)), \varphi(x,y) = \varepsilon_1 cosKx + \varepsilon_2 cosKy, \tag{9}$$

Firstly, we consider a 1D sinusoidal phase profile $\varphi(x,y) = \varepsilon\cos(Kx)$ by setting $\varepsilon_2 = 0$, $\varepsilon_1 = \varepsilon = 0.2$, as it is displayed in Fig. 5(a). In Fig. 5(b) we show the motion of two cavity solitons in presence of this holding beam. It is well known [7] that CSs approach the nearest maximum of the phase profile, hence initially the CSs move to their closest phase maxima, then they continue their thermal motion in the y direction, in which no phase modulation is present.

For both cases, with and without the phase modulation in the holding beam, the cavity soliton velocity was measured. In absence of phase modulation we obtain $v \cong 47\mu m/\mu s$, while in presence the phase modulation we get $v \cong 48.4\mu m/\mu s$. Hence the drift velocity does not seem to be significantly affected by the presence of the modulation, whose effect is thus mainly of steering the CS in the initial phase of the drift.

In another simulation, we control the CS motion by using a holding beam with an amplitude modulation. For this purpose two Gaussian beams created in the grid center were superimposed, one with phase equal to zero and waist equal to σ_1, the other with phase equal to π and width equal to σ_2, with $\sigma_1 > \sigma_2$. The amplitudes of the two Gaussian beams have been taken equal.

The result of this superposition is a beam with an amplitude gradient that has the shape of a ring (like a doughnut mode), as shown in Fig. 6(a), but in this case no phase gradient is present.

The CS is once again trapped in a circle but now it moves spontaneously because of thermal effects and it is confined to the ring (see Fig. 6(b)) by the amplitude modulation. In the case of Fig. 1, on the contrary, the CS was moving because of the phase modulation of the doughnut-shaped holding beam.

Finally, we studied the case of HB with a pure 2D phase modulation, which corresponds to $\varepsilon_1 = \varepsilon_2 = \varepsilon$ in Eq. 9 (see Fig. 7(a)). The cavity soliton moves towards the nearest maximum of the phase landscape and remains trapped there for a while. When the CS is trapped, a minimum of temperature develops in the location of the optical spot and tends to destabilize it. In Ref. [14] we showed (1D simulation) that the CS can be trapped at a phase maximum, momentarily or indefinitely, depending on the strength of the phase modulation. If this is too high, the CS dies.

In Figs. 7(b) and 7(c) we show the dynamics of the field intensity profile and of the temperature profile, respectively, for $\varepsilon = 0.05$. The optical spot starts moving and is momentarily captured by one of the nearest phase maxima where, however, the temperature field starts digging a dip which, in this case, is capable of expelling the CS. As a consequence, the CS is captured by another phase maximum for a while, then it is again expelled, and the process repeats again and again, generating random walk in the phase landscape, in a sense similar to a

#3247 - $15.00 US Received October 30, 2003; Revised December 19, 2003

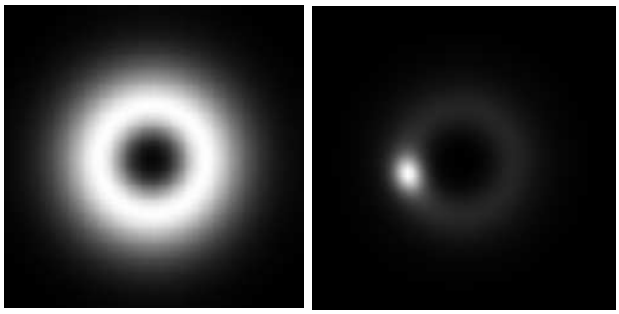

Fig. 6. The profile of the input holding beam with ring-shaped pure amplitude gradient is shown in (a). The movie (b) illustrates the motion of CS. Parameters are as in Fig. 4.

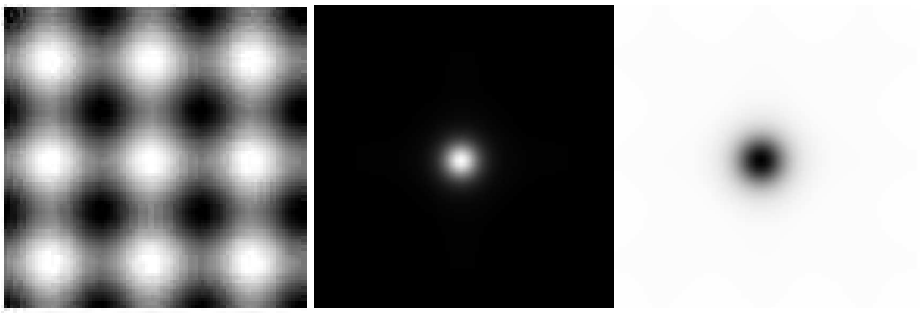

Fig. 7. 2D phase profile of the holding beam (a). The movie shows the time evolution of field intensity (b) and temperature (c). Parameters are as in Fig. 4.

slow pinball game.

4. Conclusions and discussion

The motion of CSs in presence of phase or intensity gradients is interesting for applications such as all-optical encoding and processing of information and also controlled motion of small molecules or optical tweezers.

In particular, we have shown the circular motion of CSs in presence of a TEM_{10}^{*} or a TEM_{01}^{*} mode as holding beam, both in the case of passive and active configurations, in absence of thermal effects.

We have also demonstrated that the spontaneous drift induced by thermal effects on CS can be controlled by using holding beams with phase or amplitude modulations. A peculiar phenomenon has been shown in the case of 2D phase modulation: for suitable values of the modulation amplitude, the combination of the thermally induced motion and of the attracting action of the maxima of the phase profile gives rise to a random walk in which the the CS visits in sequence the various maxima. Each jump from one maximum to another is induced by the fact that the optical spot escapes from the dip that the temperature develops at its location. This picture induces us to describe the spontaneous motion of CS, caused by the temperature dynamics, with the name “Fugitive Soliton”. Quite interesting is that the random character of the motion is not introduced by stochastic terms in the equations, but by casual choice of the speed direction of the cavity soliton in its thermally induced motion.

#3247 - $15.00 US Received October 30, 2003; Revised December 19, 2003

Acknowledgments

This work was carried out in the framework of the PRIN project *Formazione e controllo di solitoni di cavità in microrisonatori a semiconduttore* of the Italian MIUR, and the European Network VISTA (*VCSELs for Information Society Technology Applications*).

Reza Kheradmand undertook this work with the support of the " ICTP Programme for Training and Research in Italian Laboratories, Trieste, Italy ".

#3247 - $15.00 US Received October 30, 2003; Revised December 19, 2003